ORIGINAL ARTICLE

Design of ear-contactless stethoscope and improvement in the performance of deep learning based on CNN to classify the heart sound

Tanmay Sinha Roy[1] · Joyanta Kumar Roy[2] · Nirupama Mandal[3]

Abstract

Cardiac-related disorders are rapidly growing throughout the world. Accurate classification of cardiovascular diseases is an important research topic in healthcare. During COVID-19, auscultating heart sounds was challenging as health workers and doctors wear protective clothing, and direct contact with patients can spread the outbreak. Thus, contactless auscultation of heart sound is necessary. In this paper, a low-cost ear contactless stethoscope is designed where auscultation is done with the help of a bluetooth-enabled micro speaker instead of an earpiece. The PCG recordings are further compared with other standard electronic stethoscopes like Littman 3 M. This work is made to improve the performance of deep learning-based classifiers like recurrent neural networks (RNN) and convolutional neural networks (CNN) for different valvular heart problems using tuning of hyperparameters like learning rate of optimizers, dropout rate, and hidden layer. Hyper-parameter tuning is used to optimize the performances of various deep learning models and their learning curves for real-time analysis. The acoustic, time, and frequency domain features are used in this research. The investigation is made on the heart sounds of normal and diseased patients available from the standard data repository to train the software models. The proposed CNN-based inception network model achieved an accuracy of $99.65 \pm 0.06\%$ on the test dataset with a sensitivity of $98.8 \pm 0.05\%$ and specificity of $98.2 \pm 0.19\%$. The proposed hybrid CNN-RNN architecture attained $91.17 \pm 0.03\%$ accuracy on test data after hyperparameter optimization, whereas the LSTM-based RNN model achieved $82.32 \pm 0.11\%$ accuracy. Finally, the evaluated results were compared with machine learning algorithms, and the improved CNN-based Inception Net model is the most effective among others.

1 Introduction

The heart is the primary organ of the human circulatory system. The blood circulation within the heart makes the sound. The sounds come from the closing and opening of the atrioventricular valves. As these valves open and close, allowing blood flow to and from the Heart, it produces the heartbeat sound in this course. Analysis of heart sounds is fundamental to detecting any heart-related disorders. Under the investigation of heart sounds, the classification of heart-related disease is also crucial for quickly taking the correct preventive action. In practice, the background noise signals must be removed in the valvular heart disease [1, 2] analysis after receiving auscultation through an electronic acoustic stethoscope. Then the noise-free heart sound was digitized for computational needs. Convenient feature-extracting algorithms [1, 3] are applied in the computational intelligence to extract the essential features to classify the heart sound [1, 4] for diseases. As PCG signals are produced from the opening and closing of valves, they are repetitive and mechanical vibrations that

✉ Tanmay Sinha Roy
tanmoysinha.roy@gmail.com

1   Department of Electrical Engineering, Haldia Institute of Technology, Haldia, West Bengal, India

2   Eureka Scientech Research Foundation, Kolkata, India

3   Department of Electronics Engineering, Indian Institute of Technology (ISM), Dhanbad, India

occur at certain fixed time intervals and are analogous to an electrical signal. The heart sound can be analyzed in the conventional time and frequency domain using different developed algorithms and tools applied in various computational intelligence techniques. Artificial intelligence with computational intelligence plays a significant role in cardiac monitoring, early screening, and identification of valvular heart diseases. Inception networks and residual networks found suitable applications in heart sound analysis in terms of their accuracy and low screening time. Integration of squeeze and excitation blocks with these networks improved their performance depending on their respective connection positions. Detailed studies based on multiple hyperparameters are required to enhance the performance of the suitable deep-learning classifier on normal and abnormal heart sounds. Tuning hyperparameters in deep neural network models is necessary to avoid overfitting and underfitting issues. The study aims to search for the best cost-effective, simplified, and improved classifier tool for the early screening of heart diseases.

2 Paper organization

Section 3 provides a literature study of different deep learning methods used in heart sound analysis. Section 4 provides the objective of the research work. Section 5 details about techniques and materials used in this research paper. Section 6 explains the hardware development of the proposed system. Section 7 explains software based developed deep learning models for the proposed method and their improvements using hyperparameter tuning. Section 8 highlights the result analysis of the research work. Eventually, Section 9 summarizes the conclusions and future scope.

3 Related work

In this research, the signal classification of valvular heart diseases using a deep learning model is essential. According to a literature survey, many researchers have

Table 1 Recent work done on PCG signal analysis and deep learning-based methods

S. No	Reference	Method	Features used	Segmentation	Optimizer	Types of heart sound	Accuracy on test dataset
1	Deng et al., 2020 [30]	CNN+RNN	Improved MFCC	No	Adam	N A	98.01%
2	Abduh et al., 2019 [29]	2D-DNN	MFSC	No	Adam	N, A	95.50%
3	Tarik Alafif et al., 2020 [23]	2D-CNN+transfer learning	MFCC	No	SGD	N, A	89.50%
4	Cheng et al., 2019 [22]	2D-CNN	Spectrograms	No	SGD	N, A	88.00%
5	Fatih et al., 2019 [16]	2D-CNN	Spectrograms	No	Adam	N, M, EXT	80.00%
6	Xiao et al., 2020 [18]	1D-CNN	1D time-series signals	No	SGD	N, A	93.00%
7	Khan et al., 2020 [24]	LSTM	MFCC	No	Adam	N, A	91.39%
8	Raza et al., 2018 [25]	LSTM	1D time-series signals	No	Adam	N, M, EXT	80.80%
9	Ryu et al.,2016 [26]	1D-CNN	1D time-series signals	No	SGD	N, A	87.75%
10	Rubin et al., 2016 [31]	2D-CNN	MFCC	Yes	Adam	N, A	95.21%
11	Maknickas et al., 2017 [36]	2D-CNN	MFSC	No	RMSprop	N, A	87.66%
12	Li et al., 2019 [37]	1D -CNN	Spectrograms	No	Adam	N, A	96.48%
13	Wu et al., 2019 [45]	Ensemble CNN	Spectro-grams+MFSC +MFCC	No	Adam	N, A	87.91%
14	Yang et al., 2016 [39]	RNN	1D time-series signals	No	SGD	N, A	82.87%
15	Yaseen et al., 2018 [50]	SVM+DNN	MFCC+DWT	No	Adam	Normal MR, MVP, MS, and AS	87.08%

N, normal heart sounds; *M*, murmur heart sounds; *EXT*, extra systole heart sounds; *AS*, aortic stenosis; *MS*, mitral stenosis; *MR*, mitral regurgitation; *MVP*, mitral valve prolapse; *MS*, mitral stenosis

worked in this area. The authors [1] 2005 did work on different stages in heart sound signal for PCG signal analysis.

The authors [3] 2009 did work on heart sound analysis using an adaptive fuzzy inference system based on a Mamdani-type fuzzy inference classifier. The experiment was carried out on a standard heart sound repository. It was an offline method and not tested with human subjects. The authors [5] 2013 did work on heart sound analysis using different feature extraction techniques and methods. However, no artificial intelligence was involved in this. The authors [6] (2014) reviewed the papers on the classification of PCG signals. The authors [4] (2015) researched the analysis of second heart sounds, which involves computing the length and the energy of normalized heart sounds. However, they did not classify heart sounds. The authors [7] (2018) researched PCG signal sensing using several machine-learning methods for abnormal heart sound detection. However, it was used to discriminate between different types of heart sounds.

The authors [8] in 2018 and [9] in 2013 researched PCG signal analysis using the wavelet transform method. However, it had restrictions in real-time signal analysis. The authors [10] 2015 did work on the classification of heart sounds using multimodal features and obtained an accuracy of 85%. The authors [11] (2020) researched the classification of heart sound using CNN and achieved an accuracy of 88%. The authors [12] (2017) paper investigated PCG signal analysis for murmur diagnosing using Shannon energy and obtained an accuracy of 83%. The authors [13, 14] in 2017 and 2018 did work on a simple technique for heart sound detection and identification using the Kalman filter in real-time analysis, where various feature extraction techniques were discussed. Thus, improving data science models and artificial intelligence is necessary for PCG signal analysis. Table 1 shows some of the recent works that have been done on PCG signal analysis and classification methods.

4 Objective

The main objective of this paper is to design and develop an artificial intelligence-based ear-contactless electronic stethoscope that is low-cost, portable, and accurate. The developed stethoscope can also effectively diagnose various heart sound types where auscultation occurs through a bluetooth-enabled micro speaker.

5 Methods and materials

5.1 Heart sound dataset description

The research was based on four heart sound data repositories. A massive number of heart sound data (70,000 heart sound samples) are taken from these four heart sound data repositories for training and testing purposes of the modeling. The training and testing ratio is 80:20. Similar classes' heart sounds are considered during training. The heart sound banks are the only source available on the internet used by many researchers, as the literature says. These sounds are highly authentic and reliable, as described in the following: https://github.com/yaseen21khan/Classification-of-Heart-Sound-Signal-Using-Multiple-Features [15].

Five categories of heart sound samples have been considered, as shown in Fig. 1: normal sound, mitral regurgitation, mitral stenosis, mitral valve prolapse, and atrial stenosis. Each heart sound lasts for a time duration of 5 s to 10 s and has a bandwidth of 65 Hz to 500 Hz.

Heart sound dataset 2, as shown in Fig. 2, is obtained from the classification of heart sound recordings-pascal challenge dataset B [15, 16]. Three categories of heart sounds have been considered: normal, murmur, and extra–systole.

Figure 3 details the physio net challenge training set [17, 18], comprising five training databases (A through E) containing 3126 heart sound samples.

Kaggle heartbeat sounds [19, 20] dataset consisting of normal, abnormal, noisy normal, and noisy abnormal is also used for our heart sound analysis.

Mainly, two categories of heart sounds are used for analysis: normal and abnormal.

Features [21] of the heart sound considered for the whole study have been limited to:

1. Acoustic features: MFCCs, Mel, Chroma, Contrast, and Tonnetz.
2. Time domain features: RMS, Signal Energy, Signal Power, ZCR, THD, DWT, Skewness, and Kurtosis.

| Category	No. of Samples
Normal	200
Mitral Regurgitation (MR)	200
Mitral Stenosis (MS)	200
Mitral Valve Prolapse (MVP)	200
Atrial Stenosis (AS)	200

Fig. 1 Cardiac sound dataset 1

Category	No. of Samples
Normal	320
Murmur	95
Extra-Systole	46

Fig. 2 Cardiac sound dataset 2

Category	No. of Samples	
	Normal	Abnormal
Training-A	117	292
Training-B	386	104
Training-C	07	24
Training-D	27	28
Training-E	1958	183
Training-F	80	34

Fig. 3 Cardiac sound dataset 3
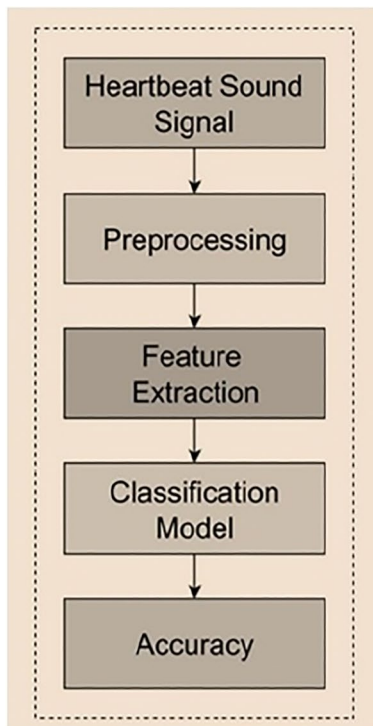
3. Time and Frequency domain features: Hilbert Huang transform (HHT)

Figure 4 depicts a block diagram of PCG signal classification [21, 22]. Heart samples are given to a pre-processing module, which applies a bandpass filter with a bandwidth of 35 to 480 Hz to suppress the ambient error. A sample length of 3 s is considered and made constant for each heart sample recording undergoing pre-processing. Various features are collected from the pre-processed heart sound, and eventually, the heart sound sample is categorized for validation of the proposed developed system.

$$x(t) = f(x(t)) \tag{1}$$

where x' (t) is the processed cardiac sound signal.

Each dataset is split into training data (85%) and test data (15%). Training data is further divided into validation data (15%) and the rest for training the model.

HHT is used as one of the feature extraction methods where the heart signal is decomposed into various intrinsic mode functions (IMFs) using empirical mode decomposition (EMD). The Hilbert transform is applied to the IMFs to obtain the time, and frequency distribution for Hilbert spectral analysis (HSA) to detect extra Heart sounds like S3 and S4.

Fig. 4 Block diagram of PCG signal classification

Process of Feature Extraction

HHT used to Detect the Presence of Murmurs, S3 & S4 Heart Sound
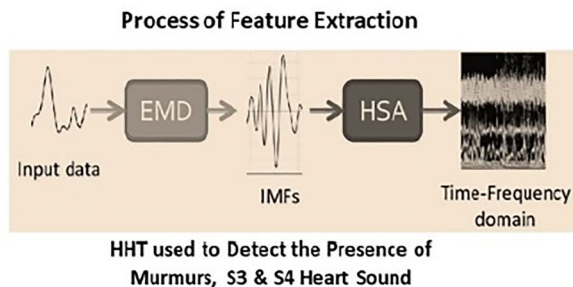
The following algorithms are applied to classify heart sounds:

1. Proposed SE-based Inception Network
2. Proposed CNN-RNN architecture
3. Proposed Recurrent Neural Network (RNN)
4. Proposed CNN-based Inception Network

All deep learning-based algorithms are written in Python ver. 3.9.2 using Thorny python editor (Linux). The proposed algorithms mentioned above are briefly described under the software development of the proposed deep learning models.

The valvular heart sounds considered for the entire PCG signal analysis [23, 24] are divided into the following categories:

1. Normal Heart Sounds
2. Mitral Stenosis
3. Aortic Stenosis
4. Mitral Regurgitation
5. Aortic Regurgitation
6. Mitral Valve Prolapse
7. Extra Systole

6 The hardware development of the proposed system

The schematic diagram of the data acquisition system and other interfaces is described in Figs. 5.

The hardware circuit for heart sound data acquisition and interface is described in Fig. 5, where it uses a chest
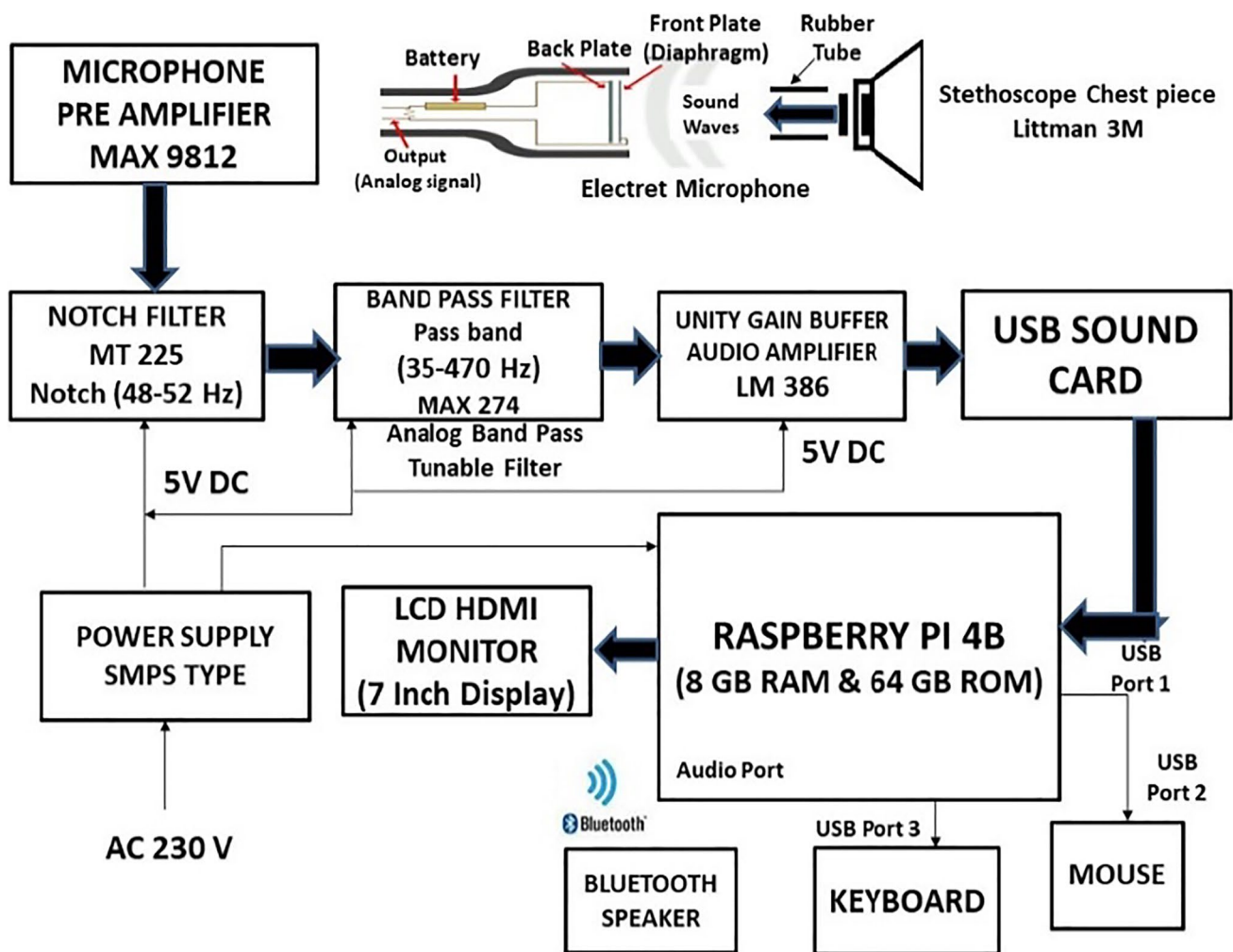

Fig. 5 Schematic diagram of the proposed heart sound acquisition system

piece for sensing real-time heart sound samples, an electret microphone for conversion of the real-time heart sounds into an electronic signal, a microphone pre-amplifier for amplification of the heart sound, a notch filter for removing the electrical interferences, an analog tunable band pass filter, a buffer amplifier for impedance matching, a Raspberry Pi 4B model acting as a CPU, a Bluetooth enabled micro speaker for listening to the captured heart sound, a power supply for the Raspberry Pi model, 7-inch touch screen for displaying the heart sound.

Heart sound in the chest generates pressure waves which the stethoscope diaphragm has picked up. The electret microphone fitted inside the chest piece and the stethoscope tube convert the heart sound signal to an electrical signal. This electrical signal is amplified by an audio amplifier based on a MAX 9812 IC chip of gain 20 and fed to the notch filter to remove electrical

interferences. The processed signal is fed to an analog tunable band pass filter with a 35–470 Hz spectrum. The heart sound signal typically [25] belongs to 35–470 Hz for normal and abnormal sounds. Finally, the processed signal is converted to digital form in a USB sound card that contains a 16-bit ADC converter with a sampling frequency of 44.1 KHz. The output of the USB sound card is connected to the Raspberry Pi 4B computer. The heart sound samples are picked up in real-time by a stethoscope sensor and saved in WAV format for further processing through the Raspberry Pi 4B with developed deep learning models. A 7-inch LCD touch screen is used to display the processed data and AI-based prediction of the disease of heart sound sample picked from the chest through the developed system in real time.

Figure 6 highlights the prototype of the proposed system incorporating all the required elements. The
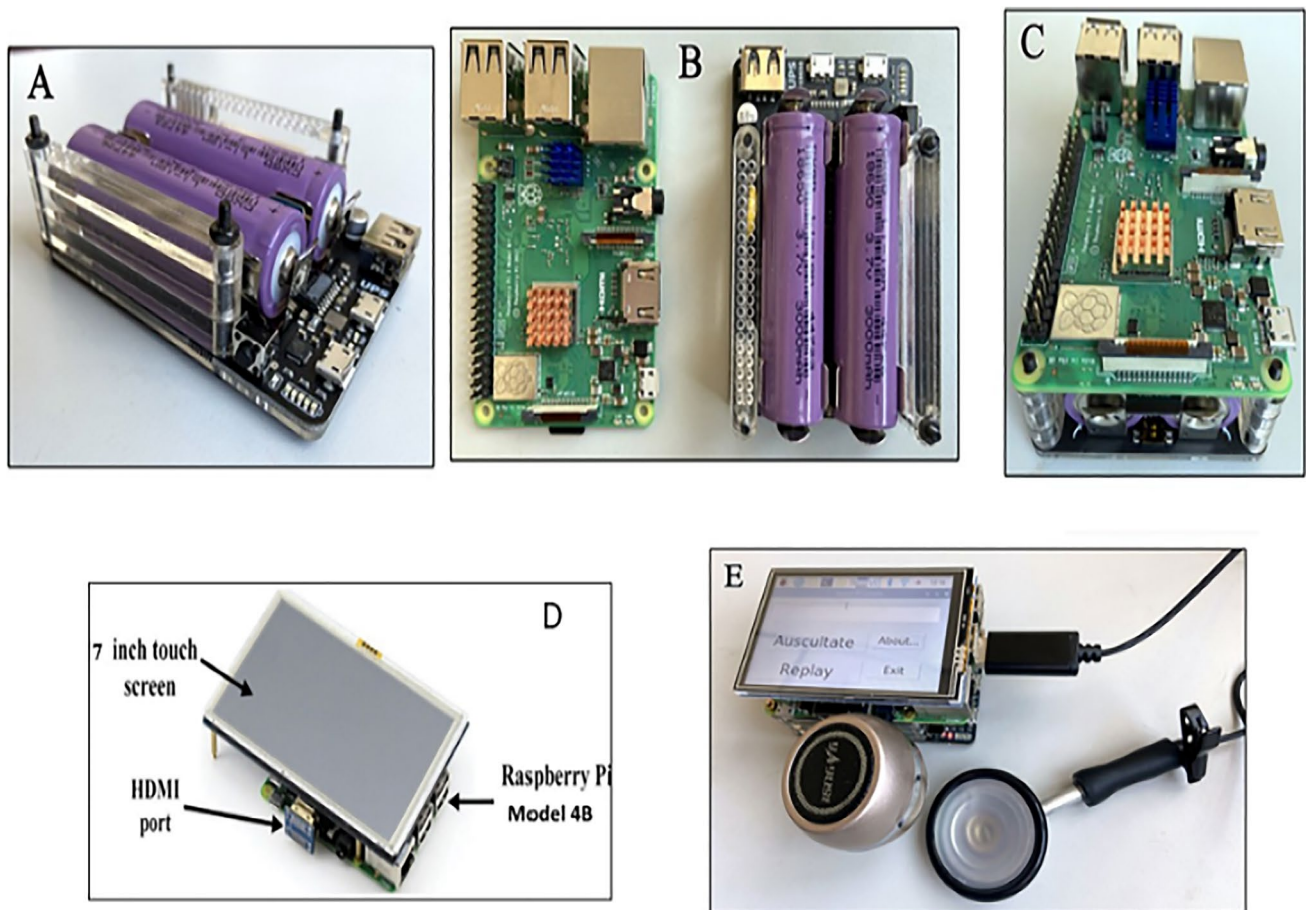

Fig. 6 The prototype of the proposed system and its components. **A** The uninterruptible power supply. **B** The Raspberry Pi 4B (left) and uninterruptible power supply (right). **C** Combination of the Raspberry Pi and the power supply. **D** A 7-inch touch screen, Raspberry Pi with power supply, and micro speaker. **E** A fully assembled device containing the components in D

Bluetooth-enabled micro speaker attached to the raspberry pi makes the stethoscope ear-contactless.

The stethoscopes are designed to meet specific parameters. The proposed stethoscope satisfies all these parameters better than others and thus can be considered an essential tool in cardiac monitoring of heart disease. Figure 7 provides the heart sounds captured in real-time through the proposed stethoscope and 3 M Littman digital stethoscope. Figure 8 provides how digital sound wav files are stored using the raspberry pi 4B model. Figure 9 shows a comparative study of the proposed stethoscope with the conventional stethoscope and 3 M Littman stethoscope based on the computation of these parameters. The third (S3) and fourth heart sounds (S4) are very low frequency and have low intensity. Thus, it can sometimes be heard using the bell of the stethoscope chest piece.

The developed system is ear contactless because heart sound plays through an external bluetooth speaker. There is no contact between the stethoscope chest piece and the ear. Therefore, it is hygienically safe during the COVID-19 chest examination. Auscultation of the heart is essential in patients with COVID-19. However, proper auscultation of these patients is difficult when medical workers wear personal protective suits.
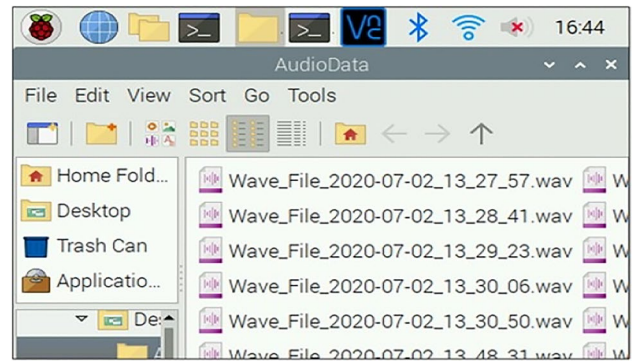

Fig. 8 Digital heart sound wav files stored in Raspberry Pi using Thorny IDE environment and Python 3.9 version

Figure 9 highlights the parameters considered in comparing the three stethoscopes:

1. Disinfection in use.
2. Ease of handling the stethoscope.
3. Safety for patients and health professionals in use.
4. Ease of auscultation.
5. Easy to afford.
6. Digital storage of wav files.
7. Compatibility with the wearing of personal protective clothing.

Fig. 7 PCG recordings obtained through 3 M Littman stethoscope and proposed stethoscope
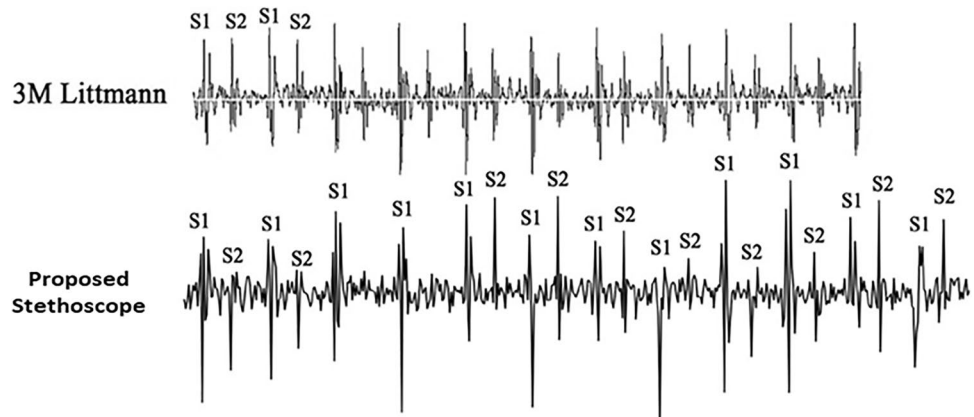
Fig. 9 Comparison of the proposed stethoscope based on the evaluation of specific parameters with a conventional stethoscope and 3 M Littman stethoscope
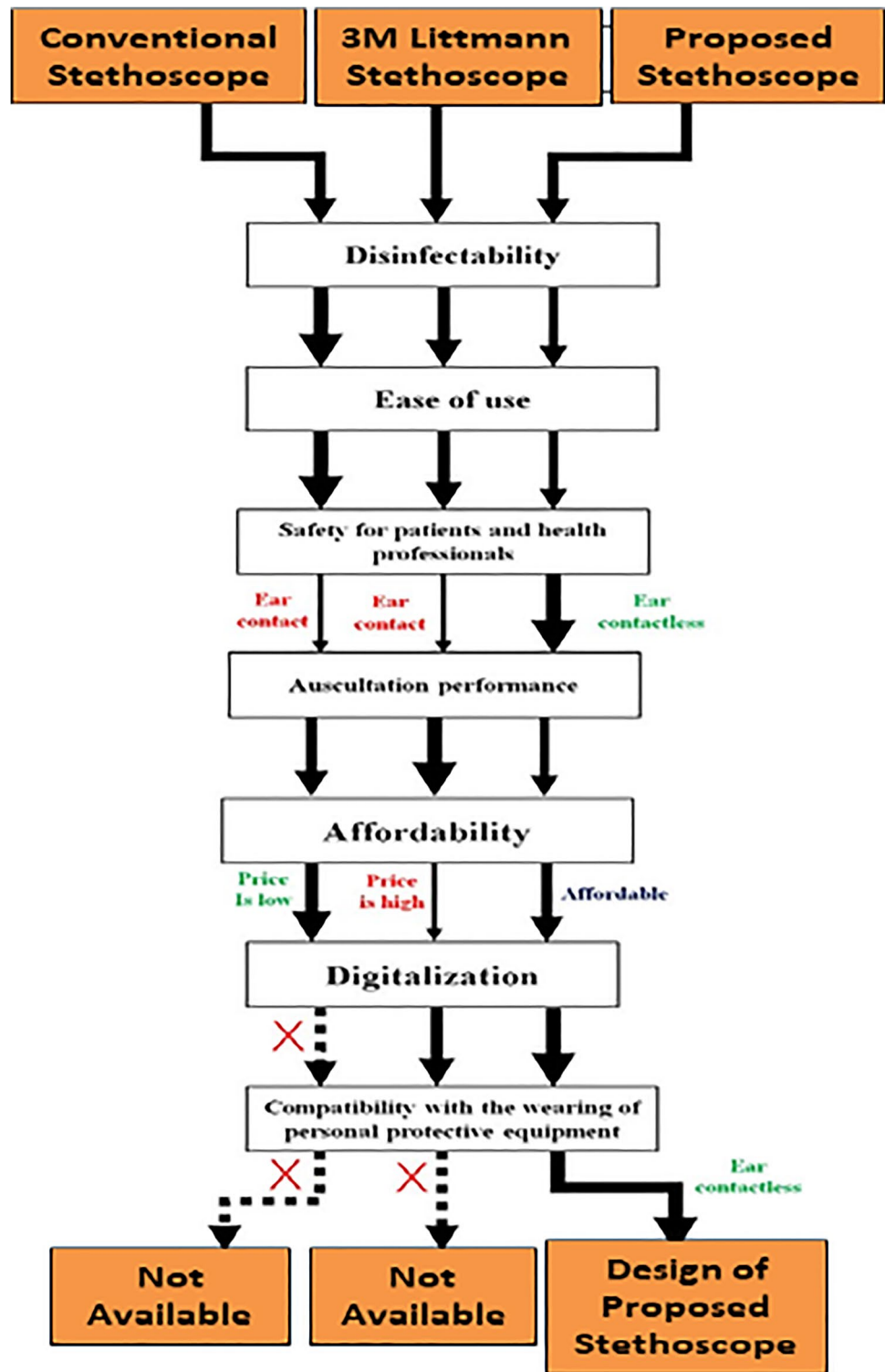
7 The software development of the proposed model

7.1 Squeeze and excitation networks applied to existing state of art architectures (SOTA)

The residual network and inception network work best for valvular heart sound analysis [26, 27]. However, their performances can be further improved by integrating squeeze and excitation (SE) blocks with the existing state of art models, as given in Figs. 10 and 11.
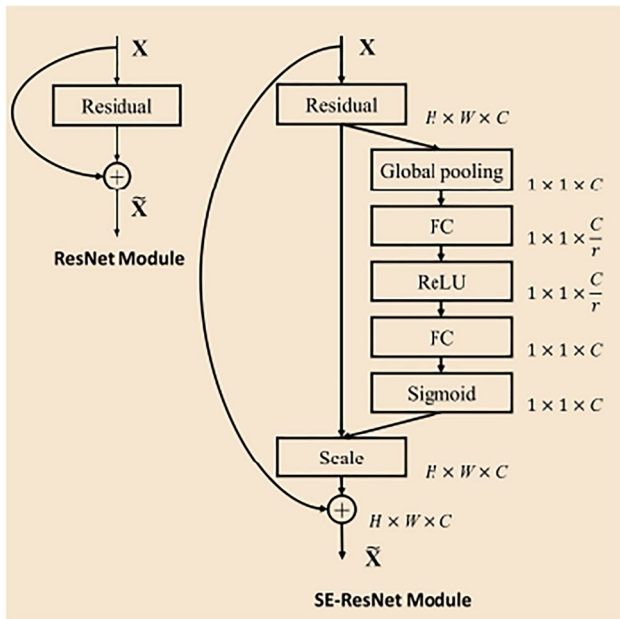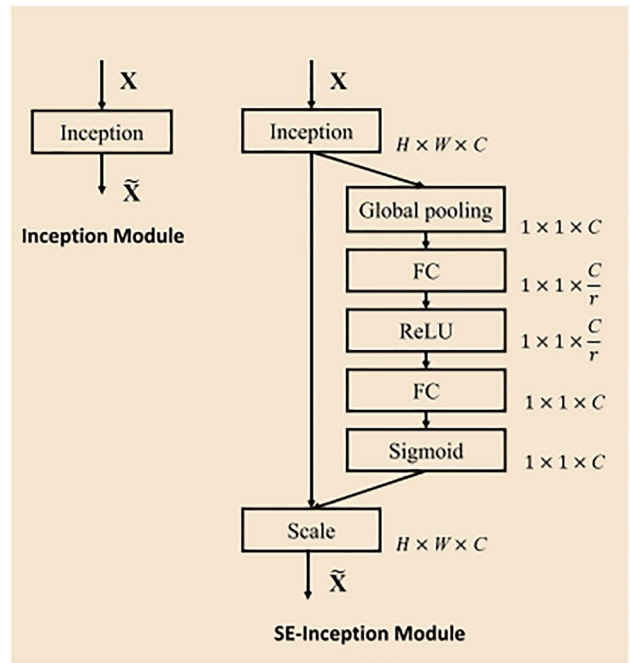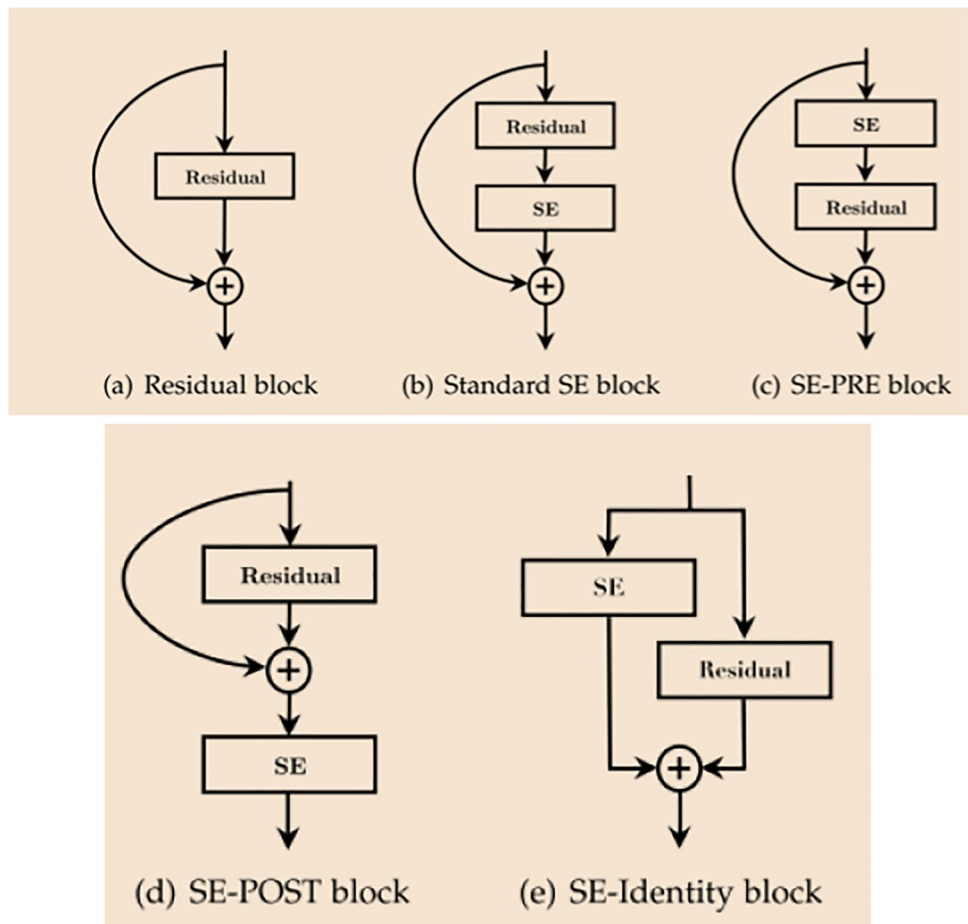
Fig. 10 SE—ResNet Block

Fig. 11 SE—Inception Net Block

Fig. 12 Various positions of squeeze and excitation blocks

(a) Residual block   (b) Standard SE block   (c) SE-PRE block

(d) SE-POST block   (e) SE-Identity block

Table 2 SE-block connection position-based results in CNN-based models applied to pascals dataset

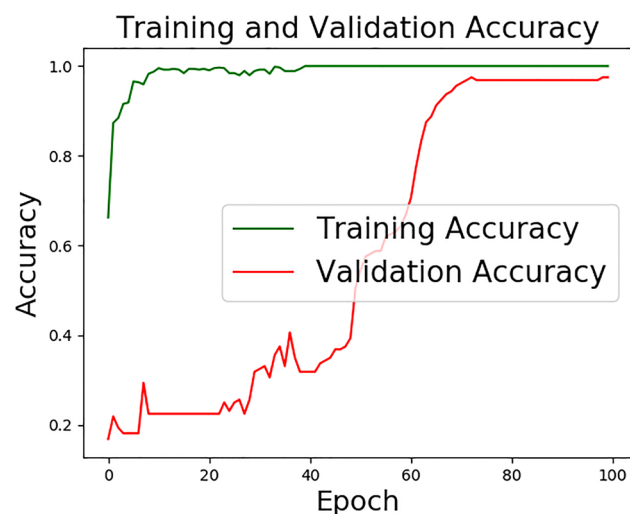| Type of module	Position	Accuracy (%)	Precision (%)	Recall (%)
ResNet	Residual Block	98.87	97.89	98.04
	Standard SE Block	99.13	98.96	98.67
	SE-Pre Block	95.67	95.32	94.56
	SE-Post Block	94.56	93.19	94.87
	SE-Identity Block	93.45	92.41	93.89
Inception Net	Inception block	98.48	98.59	97.79
	Standard SE Block	99.32	98.93	99.23
	SE-Pre Block	97.54	97.24	98.31
	SE-Post Block	95.21	94.45	93.27
	SE-Identity Block	94.37	95.67	93.68

Figure 12 provides various positions of attached SE blocks. Table 2 highlights and compares results based on the different positions of SE blocks connected with the existing CNN models. Table 2 also provides a standard SE block associated with the existing state of the model [28, 29], like inception net offers the best result among all others.

In SE modules, there exist mainly three parts:

1. Squeeze block
2. Excitation block
3. Scale block

In the squeeze block, a global average pooling operation is performed to reduce the $C \times H \times W$ shape to $C \times 1 \times 1$ shape to get a global picture for each channel.

The excitation network contains two fully connected layers, first to reduce the dimensions and second to increase
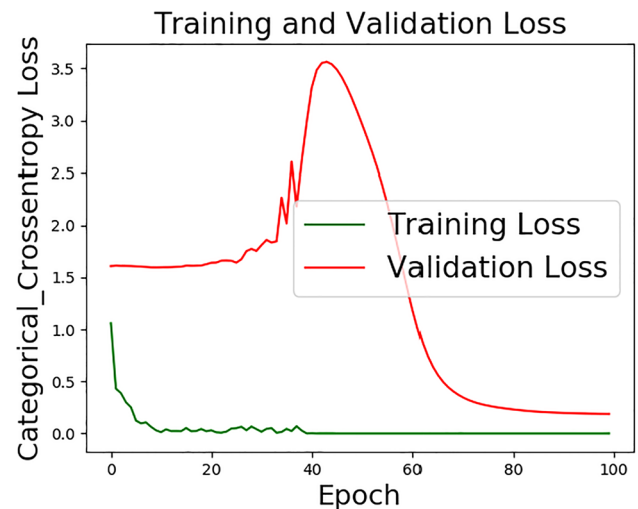
Fig. 14 Plot of cossentropy loss vs. epoch during training and validation in SE-Inception Net

the dimensions back to the original. The dimensions are reduced by a reduction ratio of $r = 16$. Initially, the vector of length C is obtained in the squeeze operation, and the next stage is to generate a set of weights for each channel which is done with the help of the excitation operation.
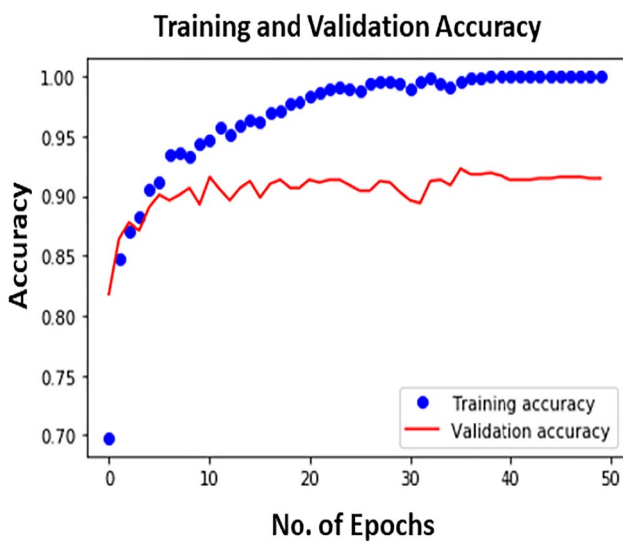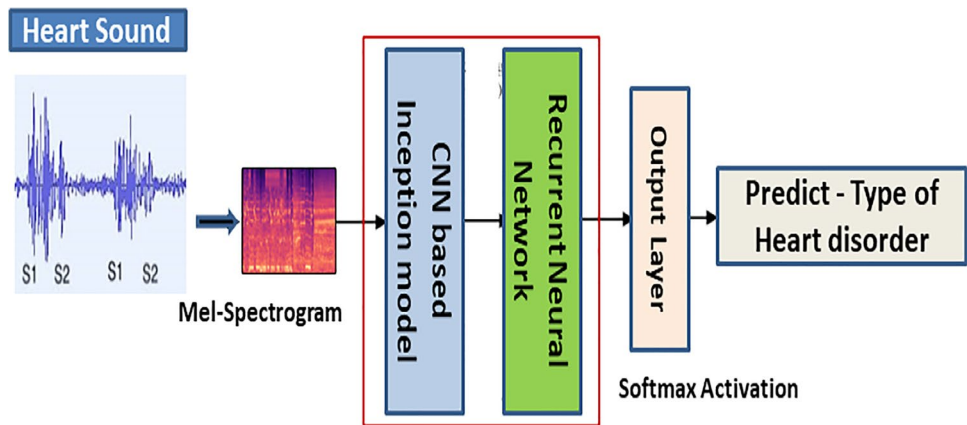
Finally, the scaling operation is done with the help of a sigmoid layer where outputs of the excitation block are multiplied element-wise with the input feature to get the final output of the SE Module.

Various learning curves are obtained, as shown in Figs. 13 and 14.

7.2 Proposed CNN-RNN architecture

A combination of CNN-RNN architecture has been proposed, where features are extracted with a CNN-based inception network, and classification is done by the RNN model, as given in Fig. 15. The hybrid CNN-based

Fig. 13 Plot of accuracy vs. epoch during training and validation in SE-Inception Net

Fig. 15 Functional block diagram of the proposed CNN-RNN model

Fig. 16 Plot of accuracy vs. epoch during training and validation

Table 3 Parameter configuration in CNN-RNN model

Hyper parameters	Candidate set	Optimized
Window length		5 s
No. of inception layers	{1,2,3,4,5,6}	6
Kernel dimensions	{3,5,7,9}	3
No. of Kernels	{32,64,128,256,512}	256
No. of LSTM layers	{1,2,3}	2
No. of hidden units	{64,96,128,256}	128
No. of epochs	{20,30,40,50}	50
Learning rate	{0.1,0.01,0.001}	0.001

LSTM, long short-term memory; Candidate Set, different set of values; Optimized, one particular selected value

inception network model and LSTM-based RNN model use some of the acoustic features of the heart sound signal like Mel-frequency cepstrum coefficients (MFCCs), Mel, Chroma, Contrast, and Tonnetz. The proposed CNN-RNN model [28, 30], after hyper-parameter settings, achieved an accuracy of 91.17%. It produced better performance in terms of accuracy compared to the RNN model after optimizing its hyperparameters.

Figure 16 depicts a plot of the accuracy of the proposed CNN-RNN model after hyper-parameter tuning with the number of epochs during the training and validation stage. It is found from the above plot that accuracy rises as the number of epochs grow.

Table 3 produces the hyper-parameter settings of the proposed model.

7.3 Proposed RNN Architecture

It is a special kind of deep neural network [13, 15] where the obtained result from the previous stage is used as input to the present stage, as explained in Fig. 17. In PCG signal analysis, it plays an important role.

$$h_t = \left(h_t - 1, x_t\right) \qquad (2)$$

where h_t = present state in RNN network.

h_{t-1} = Previous state in RNN network
x_t = Input to RNN network

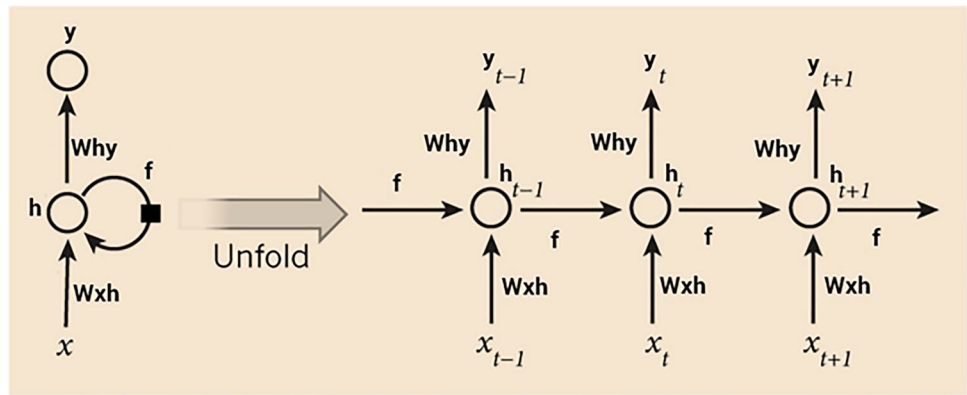$$h_t = \text{ReLU}\left(W_{hh}h_{t-1} + W_{xh}x_t\right) \qquad (3)$$

W_{hh} = Weight at recurrent neuron in RNN network
W_{xh} = Weight at input neuron in RNN network
ReLU = Activation function used in the hidden layer

$$y_t = \cdots \sigma\left(Why\ h_t\right) \qquad (4)$$

Fig. 17 Steps involved in RNN

σ   = Softmax Activation function used in the output layer

y_t = output of RNN network

W_{hy} = Weight at output layer in RNN network.

Each dataset is grouped into training data (85%) and test data (15%), as shown in Fig. 18. Furthermore, training data is decomposed into validation data (15%) and the rest for training the model. Once the proposed RNN model [31, 32] gets trained using training data, it is then validated using the validation data to adjust the hyper-parameters to get better results and choose the best-selected model. Test data is commonly used to validate the performance of the proposed model.

Fig. 18 Functional block diagram of RNN
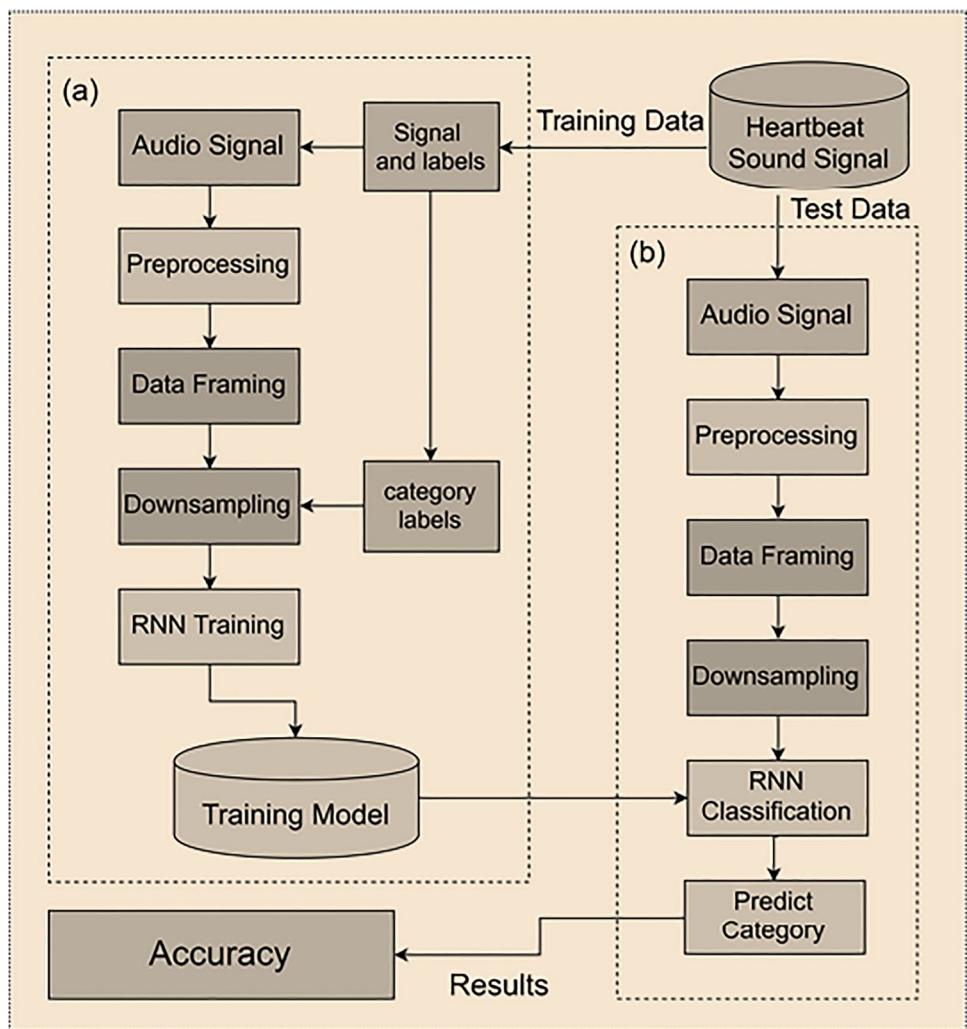
Fig. 19 Architecture of the proposed RNN using LSTM
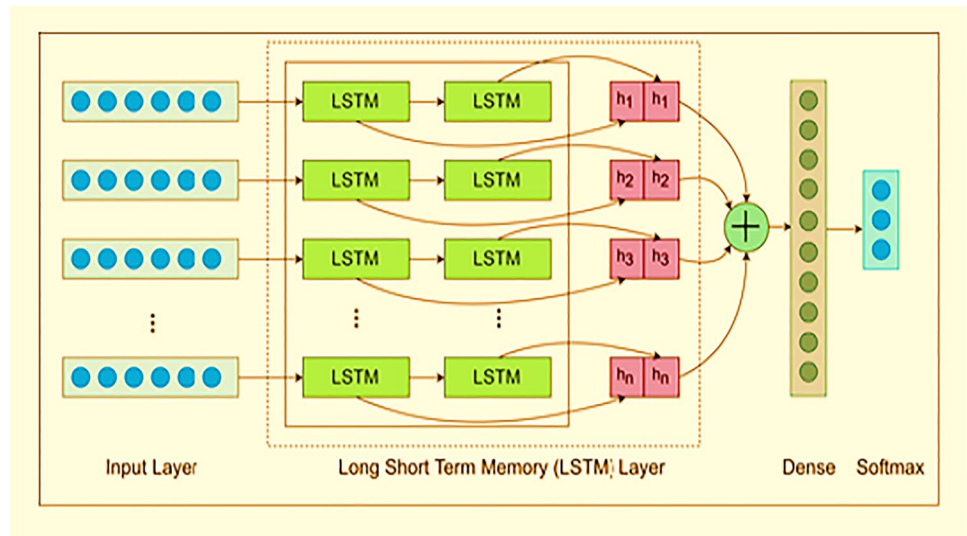
Table 4 Proposed RNN model summary

| Layer	Operator	Output height	Output width	Output depth
Input	-	01	06	01
LSTM-1	ReLU	01	06	50
Dropout	Rate = 0.35	01	06	50
LSTM-2	ReLU	01	01	20
Dropout	Rate = 0.35	01	01	20
Dense	-	01	01	03
Softmax	-	01	01	03

Eventually, statistical parameters are computed for the proposed model.

Figure 19 shows the architecture of the proposed RNN model applied to dataset 2. The input layer uses six neurons followed by two long short-term memory (LSTM) layers. The first LSTM layer [28, 33] comprises 50 neurons followed by a 35% dropout rate, whereas the second LSTM layer contains 20 neurons followed by a 35% dropout rate. In every LSTM layer, the ReLU activation function has been used. The softmax activation function has been used in the dense output layer, having several neurons depending on the dataset to which the proposed model is applied, as shown in Table 3.

Table 4 shows the proposed RNN model [34] summary using two LSTM layers with the ReLU activation function and a dense output layer with the Softmax function being used.

Figure 20 shows the cross-entropy loss [35] of the proposed RNN model under the training and validation phase. The plot of cross-entropy loss with the number of epochs indicates that loss reduces as the number of epochs rises in the training and validation stage for the proposed RNN model.
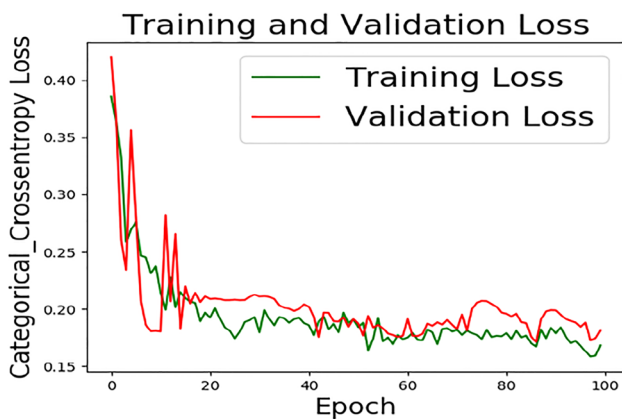
Fig. 20 Plot of cossentropy loss vs. epoch during training and validation in RNN
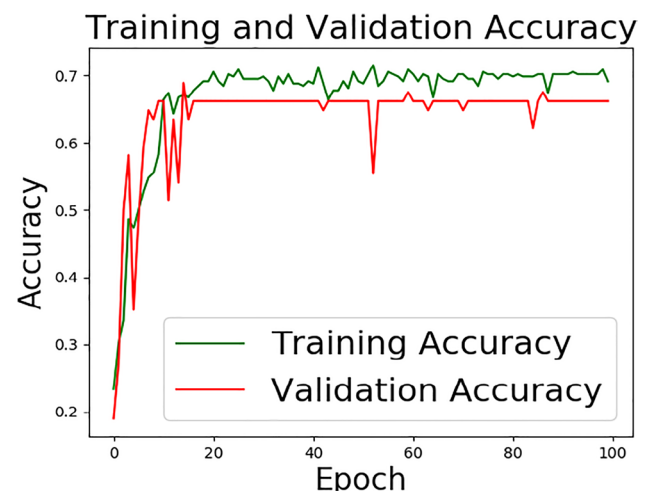
Fig. 21 Plot of accuracy vs. epoch during training and validation in RNN
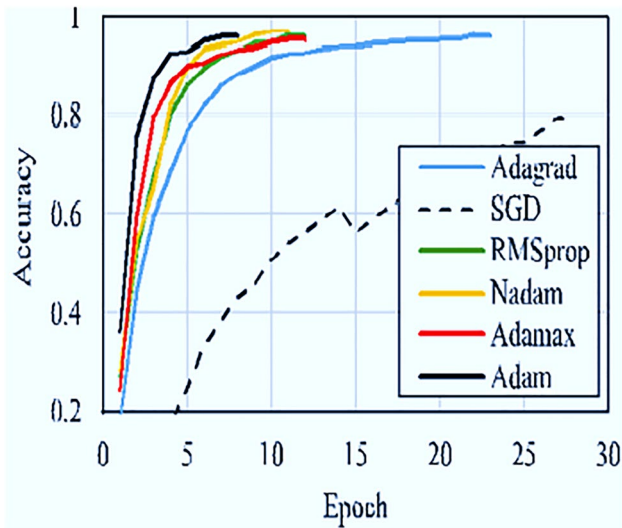
Fig. 22 Comparison of different optimizers in RNN

Table 5 Hyper-parameter tuning of samples by applying different dropout rates in RNN

Dropout rates	Accuracy	Loss
0.15	78.77	68.65
0.25	80.24	62.55
0.35	82.32	54.96

Table 6 Summary of test-data results in RNN

Model	Dropout rate	Accuracy	Precision	Recall	F1-Score
RNN	0.35	0.82	0.83	0.86	0.85

Figure 21 depicts the accuracy of the proposed RNN model under the training and validation phase. The plot of accuracy with the number of epochs indicates that accuracy rises as the number of the epochs grows in the training and validation stage for the proposed RNN model.

The effect of various optimizers on the proposed RNN model applied on dataset 2 is shown in Fig. 22. The figure below shows that the Adam optimizer gives the best result among the others.

Table 5 shows the effect of different dropout rates on the proposed RNN model. It is observed that on increasing the dropout rates, the model's accuracy increases, and cross-entropy loss decreases. The tuning of hyperparameters thus helps to choose the best proposed RNN model at a dropout rate of 0.35. The performance evaluation of the proposed RNN model is carried out on the test data by considering a drop-out rate of 35%, as shown in Table 6. After hyperparameter settings, the proposed RNN-based long short-term memory (LSTM) model achieved an accuracy of 82.32%.

Table 7 provides the block diagram of proposed Inception Net architecture. Table 8 shows the effect of adding inception blocks on the proposed inception net model. It is experimentally studied and found that increasing the number of blocks increases the model's accuracy and cross-entropy loss decreases.

Fig. 23 Effect of learning rate during training and validation using ADAM optimizer
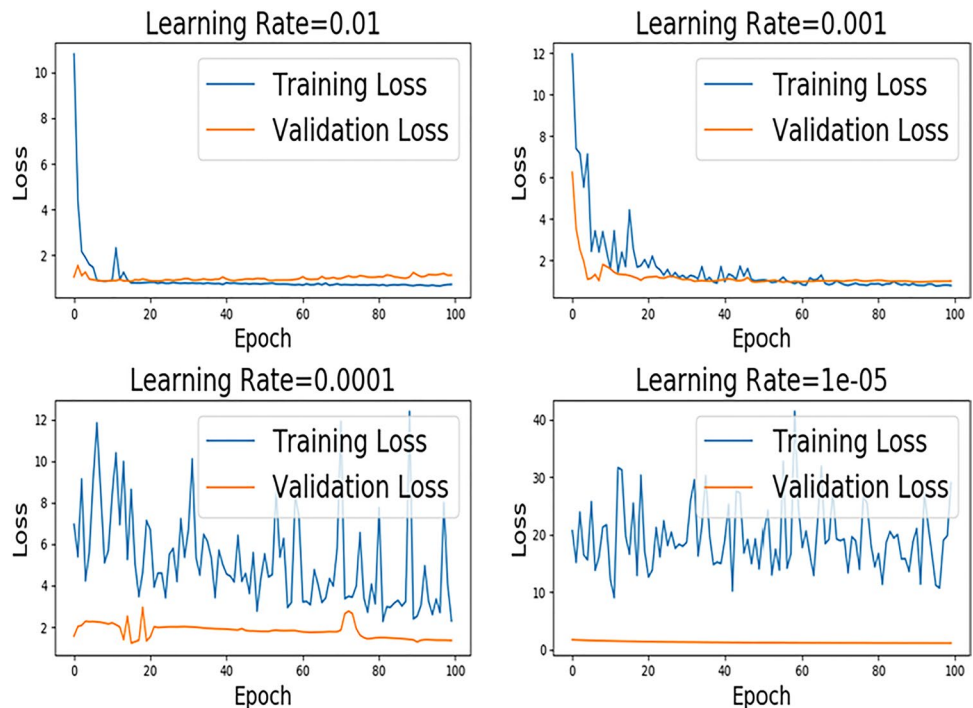
Figure 22 provides the comparative study of different optimizers used in deep learning methods like RNN. As it is clear from the above figure, the accuracy increases very steeply on implementing the said optimizer. The learning rate is a configurable and most important hyperparameter in the deep learning model. Figure 23 depicts the effect of the learning rate on the cross-entropy loss of the proposed RNN model under the training and validation phase. It shows that the optimal condition is obtained at a learning rate of 0.001. As the combined architecture of the CNN and RNN model [36, 37] has low accuracy and more training time, this hyperparameter optimization method can easily keep track of that.

Various parameters used to judge any developed system's performance are called accuracy, precision, recall, and F-measure. For the computation of these metrics, the count of true-positive (TP), false-positive (FP), true-negative (TN), and false-negative (FN) data are needed, as provided:

$$Accuracy = TP + TN/TP + FP + FN + TN \tag{5}$$

$$Precision = TP/TP + FP \tag{6}$$

$$Recall = TP/TP + FN \tag{7}$$

$$F1\ Score = 2^*(Recall * Precision)/(Recall + Precision) \tag{8}$$

7.4 Proposed CNN-based inception network

Inception networks [9, 19, 38] are often used in classification problems related to medical imaging. An inception network responds to a set of Heart sounds, performs the required operations and analysis on them, and eventually predicts the type of heart sound for classification [39]. A CNN-based inception network [40, 41] has multiple convolutional layers and inception modules to learn the various features in a heart sound and predict the class labels accordingly. All inception network parameters and hyperparameters are adjusted during the training phase of the deep learning model. A Python-based Keras sequential model [42, 43] has been taken for implementation. The entire design of the deep learning model is shown in Fig. 24. This model summary was obtained after training and validation of the dataset.

Figure 25 provides the skeleton of an inception module used. It is a sparsely connected network with a max pool and multiple convolutions of kernel sizes 1, 3, and 5 at the same layer, followed by an application of concatenation operation from all filter outputs.

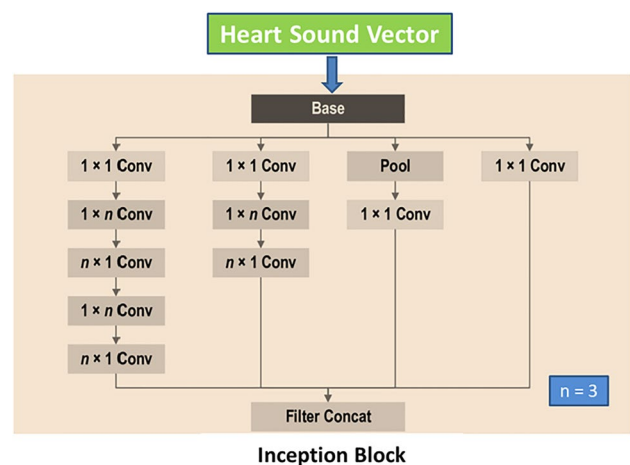**Table 7** Proposed Inception Net architecture

Type	Kernel size/stride	Activation function	Input shape
Input layer	-	-	1000×6
Conv 1D	3/1	ReLU	998×256
Conv 1D	3/1	ReLU	996×256
Dropout	0.25	ReLU	996×256
Max pool	Size = 2	ReLU	498×256
Inception block	X 3	ReLU	235×288
Dense	1200	ReLU	1×1200
Dense	600	ReLU	1×600
Dense	150	ReLU	1×150
Output layer	-	Softmax	1×5

Table 8 Effect of adding inception blocks in CNN-based Inception Net model

Inception blocks	Accuracy	Loss
01	97.85	21.00
02	98.23	19.45
03	98.79	18.05
04	99.25	16.98
05	99.45	14.87
06	99.65	12.27

Table 6 shows the proposed inception net architecture using three inception blocks with a ReLU activation function, an input layer, and an output layer with a softmax activation function.

Table 7 reflects the architecture of the proposed inception net model applied to dataset1. In this model, the first hidden convolution layer contains 256 filters,

Fig. 24 Inception net block

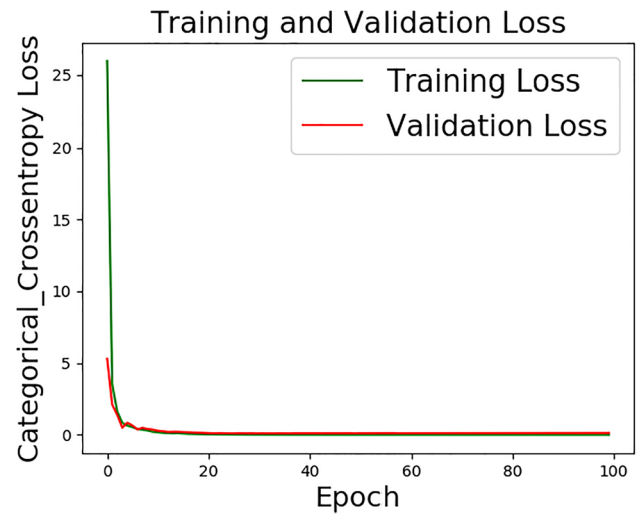**Fig. 26** Plot of cross entropy loss vs. epoch during training and validation in CNN-based Inception Net

heart sounds and plotted accordingly, as shown in Figs. 26 and 27.

Figure 26 shows the cross-entropy loss of the proposed inception net model [45] under the training and validation phase. The plot of cross-entropy loss with the number of epochs indicates that loss reduces as the number of epochs rises in the training and validation phase for the proposed inception net model. Learning rate affects the cross-entropy loss and accuracy as a lower learning rate needs a large number of iterations, and a larger one needs

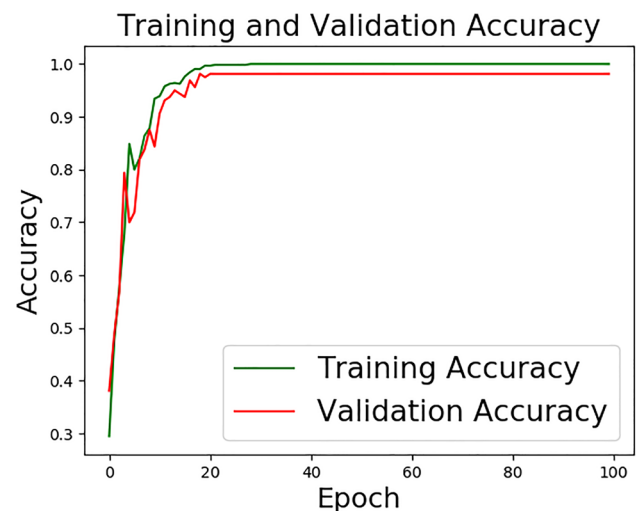**Fig. 25** Proposed CNN-based inception net model summary

each kernel size equal to 3 using the ReLU activation function, followed by the second hidden convolution layer containing the same number of filters and kernel size. The third hidden layer has three inception modules, followed by the fourth, fifth, and sixth hidden layers. They are the fully connected layer containing 1200, 600, and 150 nodes, respectively. The output layer contains five nodes using the Softmax activation function to classify five different types of heart sound [2, 44]. Learning curves are obtained for the proposed model developed with normal and abnormal

Fig. 27 Plot of accuracy vs. epoch during training and validation in CNN-based Inception Net

Fig. 28 Effect of learning rate during training and validation using ADAM optimizer
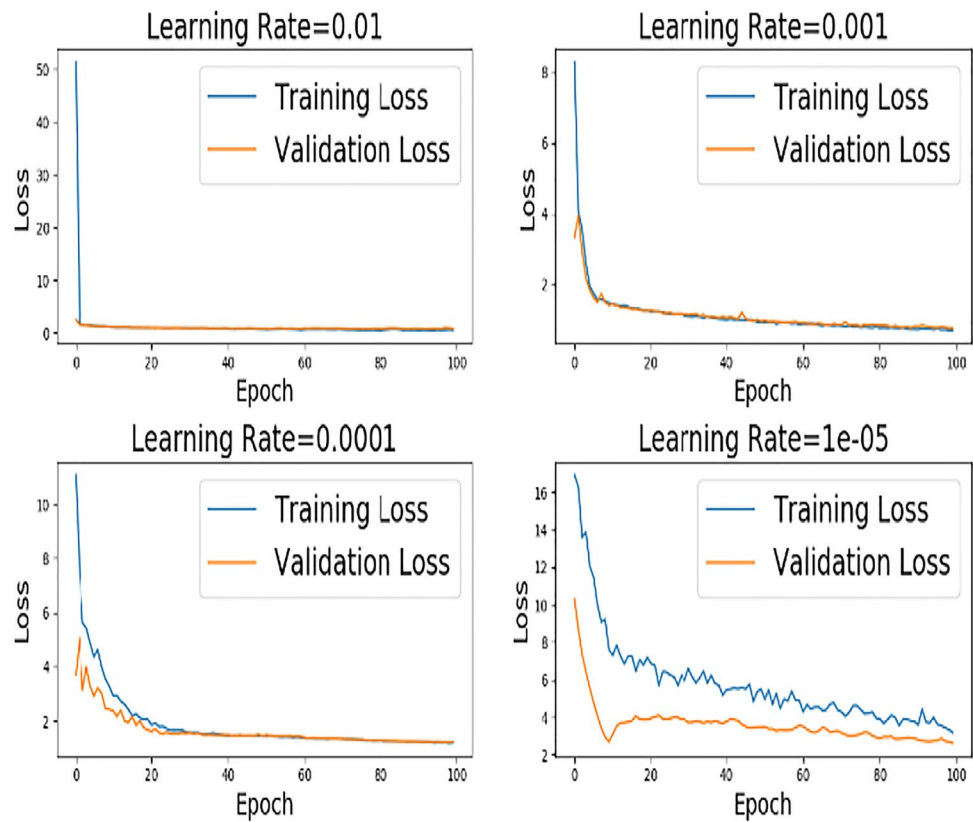
Table 9 Summary of test-data results in the Inception Network

Model	No. of blocks	Accuracy (%)	Precision (%)	Recall (%)	F1-Score (%)
Inception Net	06	99.37	97.26	98.08	99.07

a small number of iterations. Thus, choosing a proper learning rate value is a challenging and significant task, as shown in Fig. 28.

Figure 27 highlights the accuracy of the proposed inception net model under the training and validation phase. The plot of accuracy with the number of epochs indicates that accuracy rises as the number of epochs grows in the training and validation stage for the proposed CNN model.

The proposed inception net model's performance evaluation [46, 47] is carried out on the test data by selecting the number of inception blocks as six, as shown in Table 9. The best-proposed model has been chosen when the number of added blocks equals six.

Figure 28 shows the effect of the learning rate on the cross-entropy loss of the proposed inception net model

under the training and validation phase. It shows that the optimal condition is obtained at a learning rate of 0.001.

After hyperparameter settings, the proposed CNN-based inception net model achieved an accuracy of 99.65%.

7.5 Comparison to machine learning methods

The proposed model gets compared with the available machine-learning methods. A similar set of feature learning methods is considered and then a perception is made about the proposed software base deep learning model.

Dataset 1, dataset 2, and dataset 3 have been used to compare all the machine learning algorithms, as shown in Fig. 29. All machine learning algorithms [14], like Support Vector Machine [43], K-Nearest Neighborhood, Naïve Bayes, and Random Forest, are written in Python ver. 3.8 using Keras and tensor flow. Datasets have been fed to these various machine learning models using five-fold cross-validation to evaluate their performance and statistical analysis [48, 49]. Different models have been assessed against three datasets and compared, as given in the figure below. It is found that the inception network works best among all other machine learning algorithms, as shown in Fig. 30.

Fig. 29 The comparison of the machine learning performance between the proposed method (RNN and CNN) and other machine learning
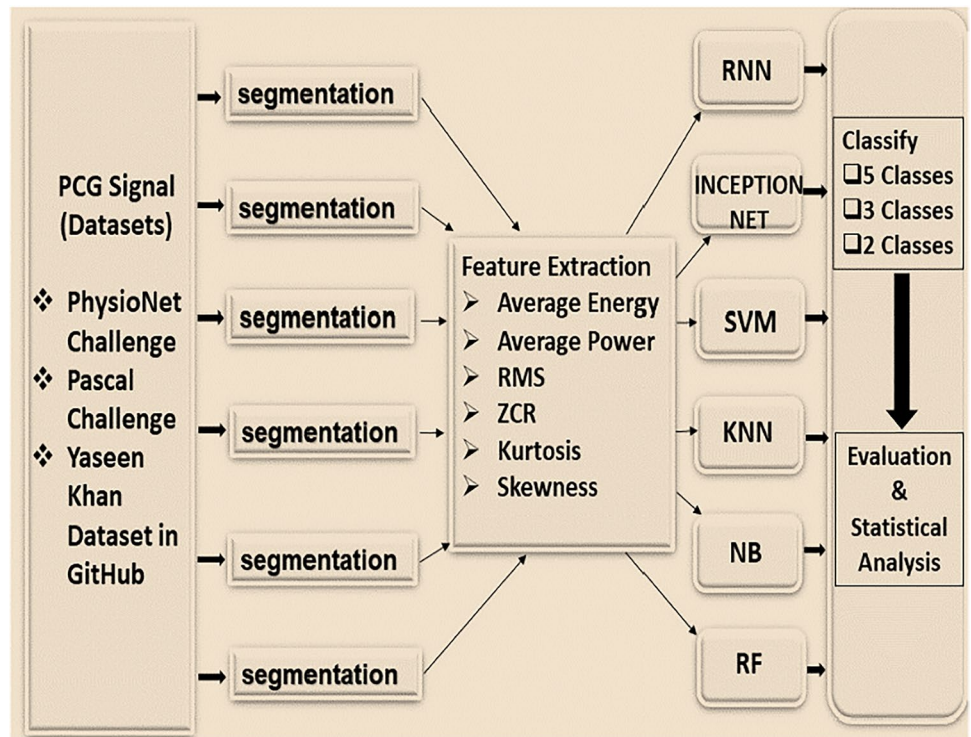
Fig. 30 Comparison of different machine learning methods with deep learning on various datasets
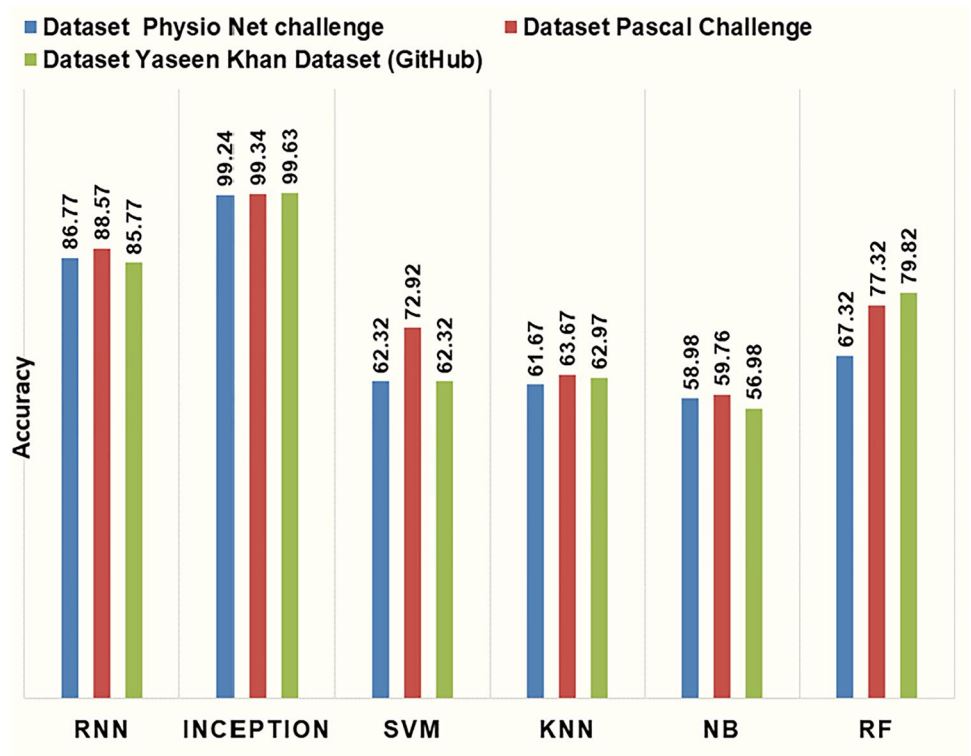
8 Result analysis

Table 10 shows the accuracy of the four proposed models. The proposed hybrid CNN-RNN model attained better accuracy after hyperparameter settings than the RNN model. It has been found that the SE-based inception network works the best of all.

Tables 11 and 12 depicts the comparison of performance metrics in terms of training time and testing time. After optimizing hyperparameters, the training time and testing time of the proposed hybrid CNN-RNN model are lower than the RNN model, and the SE-inception network achieved the most down screening time among them. Table 12 provides a detailed comparative study of the performance of different stethoscopes.

Table 13 describes the detail of the 30 volunteers of different age groups and genders considered for the entire experimental study. Table 14 analyzes PCG recordings obtained using the proposed contactless stethoscope by adapting SE-inception network. Different positions like upper left sternal border (ULSB), upper right sternal border (URSB), and lower left sternal borders (LLSB) are

Table 10 Accuracy of the proposed models

Datasets accuracy (in %)	RNN	CNN + RNN	Inception Net	Se-inception net
Physio Net Challenge	82.32%	91.17%	98.65%	99.29%
Pascal Challenge	83.14%	92.75%	97.43%	99.32%
Yaseen Khan et al	80.67%	90.35%	96.25%	99.13%
Kaggle Dataset	82.45%	91.45%	96.87%	98.74%

Table 11 Comparison of screening time of different deep learning models

Datasets run time (in Sec)	RNN	CNN + RNN	Inception net	Se-inception net
Physio Net Challenge	520 s	266 s	218 s	209 s
Pascal Challenge	478 s	298 s	215 s	197 s
Yaseen Khan et al	487 s	311 s	265 s	257 s
Kaggle Dataset	357 s	293 s	220 s	206 s

Table 12 Comparison of performance metrics of different deep learning models

| Model	A (%)	P (%)	R (%)	F (%)	Training time (s)	Testing time (s)
RNN	82.32	83.11	86.05	85.80	1567	1345
RNN + CNN	92.11	93.87	92.65	93.87	1244	1174
Inception	98.65	97.45	98.65	98.05	710	974
Se–Inception	99.45	98.97	98.75	99.03	680	943

A, accuracy; *P*, precision; *R*, recall; *F*, F1-score

Table 13 Comparison of performance metrics of different stethoscopes

Data sets	Yaseen Khan dataset				Physio net challenge				Pascal challenge			
Types of stethoscopes	A (%)	P (%)	R (%)	F (%)	A (%)	P (%)	R (%)	F (%)	A (%)	P (%)	R (%)	F (%)
Type-A	95	94	93	95	94	93	92	94	94	95	94	93
Type-B	96	95	94	95	96	94	95	96	96	95	96	95
Type-C	98	97	98	99	97	98	98	97	98	97	99	98

A, accuracy, *P*, precision; *R*, recall; *F*, F1-score; *Type A*, conventional stethoscope; *Type B*, 3 M Littmann stethoscope; *Type C*, proposed stethoscope

Table 14 Description of the volunteers considered

AGE	Age group	Male	Female	Number of volunteers
25–40	Young adults	09	06	15
41–60	Middle aged adults	07	05	12
61–80	Old adults	02	01	03
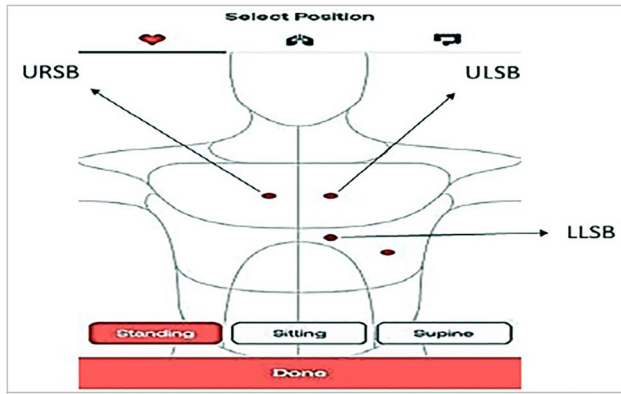
Fig. 31 Locations of heart for the acquisition of heart sound

considered for this analysis under postures like sitting, standing, and supine. The recordings are finally compared with their past medical history.

For heart sound detection of valvular disease, the stethoscope diaphragm should be placed with good contact on the body over the heart at areas defined in Fig. 31. In the case of pulse rate measurement, the stethoscope

Table 16 Analysis OF PCG recordings obtained using the proposed stethoscope with past medical history

Patient		Comparison of probability score with past medical history		
Gender	Age	Medical history	Probability of normal heart sound	Score
Female	28	NS	61.12%	3
Male	32	NS	83.43%	5
Female	51	NS	100.00%	5
Male	59	NS	83.43%	5
Female	86	MR	61.12%	3
Male	62	MS	83.43%	5
Female	37	NS	61.12%	3
Male	36	NS	83.43%	5
Female	34	NS	83.43%	5
Male	38	NS	83.43%	5
Male	27	NS	83.43%	5
Male	46	MS	83.43%	2
Male	25	NS	83.43%	5

diaphragm is placed over bronchial arteries. The almost 30 mm Hg pressure is higher than the systolic pressure during palpation. For every volunteer, nine PCG readings (3 readings from each posture) are obtained using the developed system. Table 15 shows the scores on a 1 to 5 scale by comparing the developed stethoscope readings with the volunteer's medical history. The developed system works quite decently for most volunteers in terms of accuracy (Table 16).

Table 15 Analysis of pcg recordings obtained in various positions with different postures applied on different subjects using the proposed contactless stethoscope

Patient		Sitting			Standing			Supine			Probability Score
Gender	Age	ULSB	URSB	LLSB	ULSB	URSB	LLSB	ULSB	URSB	LLSB	NormalSound
Female	28	MR	MR	NS	NS	NS	NS	NS	MR	MR	61.12%
Male	32	NS	NS	NS	NS	NS	MR	NS	NS	MR	83.43%
Female	51	NS	NS	NS	NS	NS	NS	NS	NS	NS	100.00%
Male	59	NS	NS	NS	NS	MR	NS	MR	NS	NS	83.43%
Female	86	NS	NS	NS	MS	NS	MR	MR	NS	MR	61.12%
Male	62	NS	NS	NS	NS	NS	MR	NS	NS	MR	83.43%
Female	37	NS	MS	NS	MS	NS	NS	MR	NS	NS	61.12%
Male	36	NS	NS	NS	MR	NS	NS	MR	NS	NS	83.43%
Female	34	NS	NS	NS	MS	NS	MR	NS	NS	NS	83.43%
Male	38	MS	NS	NS	NS	NS	MR	NS	NS	NS	83.43%
Male	27	MS	NS	NS	NS	NS	MR	NS	NS	NS	83.43%
Male	46	MS	NS	NS	NS	NS	NS	NS	NS	MS	83.43%
Male	25	MR	NS	NS	NS	NS	MVP	NS	NS	NS	83.43%

NS, normal heart sounds; *EXT*, extra systole heart sounds; *AS*, aortic stenosis; *MS*, mitral stenosis; *MR*, mitral regurgitation; *MVP*, mitral valve prolapses; *ULSB*, upper left sternal border; *URSB*, upper right sternal border; *LLSB*, lower left sternal border

9 Conclusion

Machine learning algorithms have certain restrictions in real-time valvular heart sound analysis applications. This research aimed to use a CNN-based deep learning classifier to develop a low-cost portable contactless stethoscope for valvular heart disease prediction in rural places. The hardware development provides an electronic stethoscope with ear contactless that has a bluetooth-enabled speaker. The cost of an echo ultrasound 2D/3D imaging machine for cardiac imaging is around 12,000 to 15,000 USD. Our total development cost of the AI-based prototype system for detecting and predicting heart diseases is about 2500 USD. The available echo machines for cardiac imaging are portable and easy to use in rural villages. However, the developed prototype cannot image the cardiac condition. However, it can predict valvular diseases cheaply and can be incorporated into rural village applications using artificial intelligence. The designed system was experimentally evaluated for its performance with 30 human volunteers having a medical history of 27 volunteers with normal heart, two with mitral stenosis, and one with mitral regurgitation, which the physician clinically assessed. On experimentation with those human volunteers, the developed system predicts the same results. The experimental studies aimed to find a suitable and improved deep learning classifier using Python-based convolutional neural network (CNN) and recurrent neural network (RNN) on verified normal and abnormal heart sounds of three datasets, as described in the text. Integration of SE blocks with the existing state of art architecture prevailed in better performance of the inception and residual networks where standard SE blocks produced the best results, among others. The training dataset trains the deep learning model, the validation dataset is used to validate the performance of hyperparameters of the model, and the test dataset computes the model's overall performance. It has been found that the best results can be obtained from any deep learning model by tuning the hyperparameters. In this entire experiment, classifier accuracy, precision, recall, and F1-scores are evaluated with the different heart sound databases. It has also been experimentally studied and found that the CNN-based inception network model classifier can be chosen as the most effective deep learning classifier. However, it has some complexity in the computational part. A recurrent neural network (RNN) is also suitable as an AI classifier of heart sound though it takes much time in the learning phase. However, once learned, it gives a speedy result.

Declarations

References

1. CN Gupta, R Palaniappan, S Rajan, S Swaminathan, SM Krishnan (2005) "Segmentation and classification of heart sounds". International Conference: Canadian Conference on Electrical and Computer Engineering. https://doi.org/10.1109/CCECE.2005.1557305
2. Anju SK et al (2014) Detection of cardiac murmur. Int J Comput Sci Mob Comput 3(7):76–80
3. Ahmad T, Ali H, Khan S (2009) Classification of phonocardiogram using an adaptive fuzzy inference system. Comput Sci 2:609–614
4. Barma S, Chen B-W, Ji W, Jiang F, Wang J-F (2015) Measurement of duration, the energy of instantaneous-frequencies, and splits of subcomponents of the second heart sound. IEEE Trans Instrum Meas 64(7):1958–1967. https://doi.org/10.1109/TIM.2014.2383071
5. Mandeep Singh, Amandeep Cheema, "Heart sounds classification using feature extraction of phonocardiography signal," International Journal of Computer Applications, Volume 77– No.4, September 2013, ISSN NO:0975 – 8887
6. Ajay Kumar Roy, Abhishek Misal, G. R. Sinha, "Classification of PCG signals: a survey," International Journal of Computer Applications, Recent Advances in Information Technology, 2014, ISSN No: 0975 – 8887
7. Latif S, Usman M, Rana R, Qadir J (2018) Phonocardiographic sensing using deep learning for abnormal heartbeat detection. Sens J IEEE 18(22):9393–9400
8. Dewangan NK, Shukla SP, Dewangan K (2018) PCG signal analysis using discrete wavelet transform. Int J Adv Manag, Technol, Eng Sci 8:2249–7455
9. Mishra G, Biswal K, Mishra AK (2013) Denoising of heart sound signal using wavelet transform. Int J Res Eng Technol 2(4):2319–1163
10. Randhawa SK, Singh M (2015) "Classification of heart sound signals using multimodal features" Second International Symposium on Computer Vision and the internet, Elsevier. Procedeia Comput Sci 58:165–171
11. Li F, Tang H, Shang S, Mathiak K, Cong F (2020) Classification of heart sounds using convolutional neural network. Appl Sci 10:3956. https://doi.org/10.3390/app10113956
12. Othman Matin Z, Khaleel Asmaa N (2017) Phono cardiogram signal analysis for murmur diagnosing using Shannon energy envelop and sequenced DWT decomposition. J Eng Sci Technol 12(9):2393–2402

13. JK Roy & TS Roy (2017) "A simple technique for heart sound detection and real-time analysis" Proceedings of ICST 2017 held at Macquarie University Sidney, Sensing Technology (ICST), 2017. Eleventh International Conference, 4–6. https://doi.org/10.1109/ICSensT.2017.8304502.

14. JK Roy, TS Roy, N Mandal & OA Postolache (2018) "A simple technique for heart sound detection and identification using Kalman filter in real-time analysis". International Symposium Sensing And Instrumentation IoT Era (ISSI), 1-8

15. Mdhaffar A, Bouassida Rodriguez I, Charfi K, Abid L, Freisleben B (2017) CEP4HFP: complex event processing for heart failure prediction. IEEE Trans NanoBiosci 16(8):708–717. https://doi.org/10.1109/TNB.2017.2769671

16. Femir D, S¸engür A, Bajaj V, Polat K (2019) Towards the classification of Heart sounds based on convolutional deep neural network. Health Inf. Sci Syst 7:1–9

17. Your First Deep Learning Project in Python with Keras Step. https://machinelearningmastery.com/tutorial-first-neural-network-python-keras/

18. Xiao B, Xu Y, Bi X, Li W, Ma Z, Zhang J, Ma X (2020) Follow the sound of children's heart: a deep-learning-based computer-aided pediatric CHDs diagnosis system. IEEE Internet Things J 7:1994–2004

19. Bhatikar SR, DeGroff C, Mahajan RL (2005) A classifier based on the artificial neural network approach for cardiologic Auscultation in pediatrics. Artificial intelligence in medicine 33(3):251–260

20. Kaggle heartbeat sounds. https://www.kaggle.com/datasets/kinguistics/heartbeat-sounds

21. Prasad GV, Kumar PR (2015) Analysis of various DWT methods for feature extracted PCG signals. Int J Eng Res Technol 4(04). https://doi.org/10.17577/IJERTV4IS041236

22. Cheng X, Huang J, Li Y, Gui G (2019) Design and application of a laconic heart sound neural network. IEEE Access 7:124417–124425

23. Alafif T, Boulares M, Barnawi A, Alafif T, Althobaiti H, Alferaidi A (2020) Normal and abnormal heart rates recognition using transfer learning. In Proceedings of the 2020 12th International Conference on Knowledge and Systems Engineering (KSE), 2020 275–280

24. Khan FA, Abid A, Khan MS (2020) Automatic heart sound classification from segmented/unsegmented phonocardiogram signals using time and frequency features. Physiol Meas 41:055006. https://doi.org/10.1088/1361-6579/ab8770

25. Raza A, Mehmood A, Ullah S, Ahmad M, Choi GS, On BW (2019) Heartbeat sound signal classification using deep learning. Sensors 19(21):4819. https://doi.org/10.3390/s19214819

26. Ryu H, Park J, Shin H (2016) Classification of heart sound recordings using convolution neural network. In Proceedings of the 2016 Computing in Cardiology Conference (CinC). 1153–1156

27. DB Springer, L Tarassenko, and GD Clifford (2014) Support vector machine hidden semi Markov model-based heart sound segmentation. Comput Cardiol, 625–628

28. El-Segaier M, Lilja O, Lukkarinen S, Sörnmo L, Seppanen R, Pesonen E (2005) Computer-based detection and analysis of heart sound and murmur. Ann Biomed Eng 33(7):937–42. http://www.ncbi.nlm.nih.gov/pubmed/16060534

29. Abduh Z, Nehary EA, Wahed MA, Kadah YM (2019) Classification of Heart sounds using fractional fourier transform based mel-frequency spectral coefficients and traditional classifiers. Biomed Signal Process Control 9:1–8

30. Deng M, Meng T, Cao J, Wang S, Zhang J, Fan H (2020) Heart sound classification based on improved MFCC features and convolutional recurrent neural networks. Neural Netw 130:22–32

31. Rubin J, Abreu R, Ganguli A, Nelaturi S, Matei I, Sricharan K (2016) Classifying heart sound recordings using deep convolutional neural networks and mel-frequency cepstral coefficients. In Proceedings of the 2016 Computing in Cardiology Conference (CinC), 813–816

32. Tang H, Dai Z, Jiang Y, Li T, Liu C (2018) PCG classification using multidomain features and SVM classifier. BioMed Res Int 2018:1–14. https://doi.org/10.1155/2018/4205027

33. Liu C, Springer D, Li Q, Moody B, Juan RA, Chorro FJ, Castells F, Roig JM, Silva I, Johnson AE, Syed Z, Schmidt SE, Papadaniil CD, Hadjileontiadis L, Naseri H, Moukadem A, Dieterlen A, Brandt C, Tang H, Samieinasab M, Samieinasab MR, Sameni R, Mark RG, Clifford GD (2016) An open-access database for the evaluation of heart sound algorithms. Physiol Meas 37(12):2181–2213. https://doi.org/10.1088/0967-3334/37/12/2181

34. Nygaard H et al (1993) Assessing the severity of aortic valve stenosis by spectral analysis of cardiac murmurs (spectral vibrocardiography) Part I: Technical aspects. J Heart Valve Dis. 2(4):454–467

35. Gomes EF, Bentley PJ, Coimbra M, Pereira E, Deng Y (2013) Classifying heart sounds: approaches to the PASCAL challenge. In Proceedings of the HEALTHINF 2013- Proceedings of the International Conference on Health Informatics, Barcelona, Spain, pp 337–340

36. Maknickas V, Maknickas A (2017) Recognition of normal, abnormal phonocardiographic signals using deep convolutional neural networks and mel-frequency spectral coefficients. Physiol Meas 38:1671–1684

37. Li F, Liu M, Zhao Y, Kong L, Dong L, Liu X, Hui M (2019) Feature extraction and classification of heart sound using 1D convolutional neural networks. EURASIP J Adv Signal Process 59:1–11. https://doi.org/10.1186/s13634-019-0651-3

38. Quiroz-Juárez MA, Jiménez-Ramírez O, Vázquez-Medina R, Ryzhii E, Ryzhii M, Aragón JL (2018) Cardiac conduction model for generating 12 lead ECG signals with realistic heart rate dynamics. IEEE Trans Nanobiosci 17(4):525–532. https://doi.org/10.1109/TNB.2018.2870331

39. Yang TC, Hsieh H (2016) Classification of acoustic physiological signals based on deep learning neural networks with augmented features. In Proceedings of the 2016 Computing in Cardiology Conference (CinC), 569–572

40. Javed F, Venkatachalam PA, Ahmad Fadzil MH (2006) A signal processing module for the analysis of heart sounds and heart murmurs. J Phys: Conf Ser 34(1):1098–1105. https://doi.org/10.1088/1742-6596/34/1/181

41. Lubaib P, Ahammed Muneer KV (2016) The heart defect analysis based on PCG signals using pattern recognition techniques. Procedia Technol 24:1024–1031. https://doi.org/10.1016/j.protcy.2016.05.225

42. Muruganantham. Methods for classification of phonocardiogram. TENCON, (2003)

43. Wu JB, Zhou S, Wu Z, Wu XM (2012) Research on the method of characteristic extraction and classification of Phonocardiogram. In: 2012 International Conference on Systems and Informatics. ICSAI 2012. https://doi.org/10.1109/ICSAI.2012.6223377

44. Cheema A, Singh M (2013) Steps involved in heart sound analysis- a review of existing trends. Int J Eng Trends Technol 4(7):2921–2925

45. Wu JM-T, Tsai M-H, Huang YZ, Islam SH, Hassan MM, Alelaiwi A, Fortino G (2019) Applying an ensemble convolutional neural network with Savitzky-Golay filter to construct a phonocardiogram prediction model. Appl Soft Comput 78:29–40

46. JK Roy, TS Roy, SC Mukhopadhyay (2019) "Heart sound: detection and analytical approach towards diseases". Modern Sensing Technologies, 103–145. https://doi.org/10.1007/978-3-319-99540-3_7

47. Suo Q et al (2018) Deep patient similarity learning for personalized healthcare. IEEE Trans Nanobiosci 17(3):219–227. https://doi.org/10.1109/TNB.2018.2837622

48. S Romiti, M Vinciguerra, W Saade, I Ansocortajarena and E Cresco (2020) "Artificial intelligence and cardiovascular diseases: an unexpected alliance". Cardiol Res Pract, 2020

49. Li D, Huang M, Li X, Ruan Y, Yao L (2018) MfeCNN: mixture feature embedding convolutional neural network for data mapping. IEEE Trans Nanobiosci 17(3):165–171. https://doi.org/10.1109/TNB.2018.2841053

50. Yaseen G-Y, Kwon S (2018) Classification of heart sound signal using multiple features. Appl Sci 8:2344. https://doi.org/10.3390/app8122344

Joyanta Kumar Roy received a Ph.D. degree from Calcutta University, West Bengal. He has been an Electronics and Automation Engineer for the last forty years as a Company Director, Consulting, Engineering, Developer, Researcher, and Educationist. He is currently with the Narula Institute of Technology as a Visiting Professor and a Company Director with M /S. System Advance Technologies, and as a Freelance Consultant with several industries. He used to give design support toward intelligent technology in the water sector. His research interests include developing intelligent measurement and control systems, multifunction sensors, IoT-based health, technology-assisted living, and smart home and city. He is a Senior Member of IET, a Fellow Member of IETE and IWWA, and a regular reviewer of IEEE and Springer Journals. He is an Editor of the S2IS journal. He published many scientific and technical publications in books, book chapters, design documents, and research papers.

Tanmay Sinha Roy was born in West Bengal, India, in 1988. He received his B.Tech. Degree in Instrumentation and Control engineering from the West Bengal University of Technology, West Bengal, India, in 2009, and the M.Tech. Degree in Applied Electronics and Instrumentation Engineering from West Bengal University of Technology, India, in 2011. He is currently an Assistant Professor in Electrical Engineering, Department, Haldia Institute of Technology, West Bengal University of Technology, pursuing his Ph.D. from IIT(ISM), Dhanbad. His research interests include PCG signal analysis, developing systems for heart sound acquisition, instrumentation, and control, and designing low-cost acoustic Stethoscopes for diseased patients.

Nirupama Mandal received a Ph.D. from Calcutta University, West Bengal, in 2012. She is an Associate Professor with the Department of Electronics Engineering, Indian Institute of Technology (ISM), Dhanbad. She was a HOD with the EIE department at Asansol Engineering College, West Bengal, in 2013. She received a The National Scholarship award from the Government of India in 2001 was then elevated to IEEE senior member in February 2019. Her research interests include Transducer Development, Controller Design, Process Plant Instrumentation, Process Modeling, Smart sensing system, and intelligent instrumentation.